2020 IEEE/RSJ International Conference on Intelligent Robots and Systems (IROS)
October 25-29, 2020, Las Vegas, NV, USA (Virtual)

Online System for Dynamic Multi-contact Motion with Impact Force Based on Contact Wrench Estimation and Current-Based Torque Control

Kazuki Fukazawa[1], Naoki Hiraoka[1], Kunio Kojima[1], Shintaro Noda[1], Masahiro Bando[1], Kei Okada[1], Masayuki Inaba[1]

***Abstract*—**
Humanoid robots are expected to play a big role at distress sites and disaster sites. There is a variety of multi-contact locomotion forms other than bipedal walking such as crawling through tightly, getting on the rubble by using its knees and elbows, or jumping in and rolling over the obstacles. If such multi-contact locomotion forms can be achieved, robots can reach environments that are currently unreachable, and be able to conduct tasks required at the environments. To achieve this, it is required for robots to bring various parts of its body into contact with the environment like a human. However, it is difficult for parts without 6-axis force sensors to achieve the target force while adapting to the environment against impact force. It is also difficult to measure contact wrenches without 6-axis force sensors. In this paper, by allowing the error of the contact state, we propose online system for realizing dynamic motion which impact force occurs on the parts of the whole body by contact to the environment. In the proposed system, we applied the current-based torque control for joints to make the whole body parts of the robot adapt to the environment, and we modified motion in real time to stabilize zmp by estimating contact wrenches at the contact positions where force sensors are not mounted. In addition, at the motion planning, we generated more feasible motions for a robot applying torque control by using evolutionary computation which advances the search with the behavior of torque control. We demonstrate that the proposed system is effective by showing experimental results of sitting posture locomotion using a JAXON robot in which impact force occur on the back of the thighs which have no force sensors.

I. INTRODUCTION

Humanoid robots are expected to be active at distress sites and disaster sites which is risky and required a variety of locomotion and operation capabilities equal to or greater than human. If various multi-contact locomotion forms other than bipedal walking such as crawling through tightly, getting on the rubble by using its knees and elbows, or jumping in and rolling over the obstacles can be realized, robots can reach environments that are currently unreachable, and be able to conduct tasks required at the environments. However, not so many motions which involve contacts on body parts without force sensors have realized, because it is difficult for parts without 6-axis force sensors to achieve the target contact wrench while adapting to the environment against impact force, and also to measure the conditions of contact wrenches.

Fig. 1. Appearance of humanoid robot JAXON during locomotion in a sitting posture as a representative of dynamic multi-contact motion. The contact points are hands (with 6-axis force sensors) and thighs (without force sensors).

Among the multi-contact motions currently implemented, stepladder climbing motion [1][2], ladder climbing motion [3][4], stair climbing motion with its hand on a handrail [5], slope climbing by pulling rope by hands [6], and quadruped walking [7] are motions that limit the contact points to hands and feet which mount the 6-axis force sensor.

As motions that do not limit the contact points to the parts with force sensors, balancing motion [8] by bringing its knee in contact with the environment, which force sensors are not mounted on, is implemented by applying Henze's method [9] which is proposed to enable full-body control without contact wrench feedback for robots which torque sensors are mounted on each joint and joint torque control based on torque sensor feedback is applied. The motion of pushing and moving a heavy object using a centaur-type humanoid with torque sensors [10] is also implemented without force sensors on contact points. However, it is generally known that the sampling frequency of torque sensors is much slower than that of current sensors, and they cannot cope with impact force propagating faster than that due to the backdrivability.

As motions to contact parts where force sensors are not mounted, motions that can contact the whole body parts

[1]K. Fukazawa, N. Hiraoka, K. Kojima, S. Noda, M. Bando, K. Okada, M. Inaba are with Department of Mechano-Infomatics, The University of Tokyo, 7-3-1 Hongo, Bunkyo-ku, Tokyo 113-8656, Japan fukazawa at jsk.imi.i.u-tokyo.ac.jp

978-1-7281-6211-9/20/$31.00 ©2020 IEEE

without using torque sensors [11] have also been realized. However, since these motions are limited to static, it requires a long time to realize target motions, and the motions that can be realized are limited.

Therefore, our goal is to achieve motions that can contact the whole body parts without force sensors with respect to dynamic motions which involve impact forces. As dynamic multi-contact motions, although some are implemented such as motion from standing to kneeling [12] and forward rotation [13], parts that can be contacted and motions that can be conducted are still limited. In this paper, by applying current-based torque control and stabilizer based on contact wrench estimation extended to dynamic motion, we propose the online system for realizing dynamic motion including contact with impact force on parts of the whole body.

II. PROBLEMS FOR DYNAMIC MULTI-CONTACT MOTION WITH IMPACT FORCE

In order to realize contacts with impact force, it is necessary to realize target contact wrench adapted to the shape of the environment, while absorbing impact force to suppress damage to the hardware by impact force and propagation of the impact to the whole body. Moreover, in order to realize multi-contact motions which whole body parts can make contact with, it is necessary to appropriately acquire the state of the robot even for parts without force sensors. Unless these problems are solved, errors in the contact wrench and the contact timing cannot be tolerated in parts without force sensors.

A. Realization of Target Wrench for Whole Body Parts

As control for realizing target wrench while adapting to the environment, the compliant control according to the error between the target wrench and the actual wrench is generally applied on parts with force sensors [1],[5],[7],[11]. However, the compliant control cannot cope with impact force propagating faster than the whole body control cycle of the robot.

On the other hand, current-based torque control has higher ability to realize the target wrench while absorbing impact force and adapting to the environment because the control doesn't need whole body control feedback (only robot and joint controller (sky blue) cycle in Fig. 2) for absorbing impact force. The whole body control frequency (whole online system (blue) cycle in Fig. 2) of the robot we used is 500 [Hz], and sampling frequency of the current sensor used for each joint (ADS1208 [14] or AMC1203 [15] by Texas Instruments) are about 40 [kHz]. Current-based torque control has even more potential to cope with higher impact by applying method for compensating for backdrivability [16] or method using hardware with small backdrivability [17]. Therefore, we realize dynamic multi-contact motion by current-based torque control. However, since current-based torque control cannot keep the robot's target posture during dynamic motion due to adaptation to the environment, online modification of motion is required and there are few examples in which the control is applied in the multi-contact motion.

In this paper, we modified motion by stabilizer controlling zmp. Since the difference between target and actual posture becomes large by current-based torque control, there is a great need for motion modification by feedback. As the motion modification by zmp control, Kajita's method [18] of modifying and realizing the target zmp based on the linear inverted pendulum model is well known.

Nozawa's method [1] extended Kajita's method [18] to multi-contact and to achieve the target contact wrench of the planned motion within the range of realizing the modified zmp. However, these methods are based on the premise that there are force sensors on contact points.

B. Contact Wrench Estimation on Parts without Force Sensors

To stabilize motion by zmp control, it is required to obtain contact wrenches for all contact points. There have been many previous studies for methods for detecting and estimating external forces for parts without force sensors on robot arms [19]. As a method for detecting contact points on humanoid robot which is a floating link system, the method applying particle filter [20] has been proposed.

Hiraoka's method [11] estimates contact wrenches by reducing the mass parameter errors of the robot model by assuming that the contact points are known from the planned motion and limiting to static motion. We extend this to contact during dynamic motion in this paper.

C. Proposed System

Fig. 2 is the system overview of the proposed online system, which is for dynamic multi-contact motion with impact force by tolerating errors in the contact wrench and the contact timing even in parts without force sensors.

The following is a brief explanation of the overall flow of the system. Planned motion and required values of the motion are given from motion generator. Using the values and the feedback values, stabilizer modifies motion by zmp control. Then the target torque is calculated and given to joint layer which applied current-based torque control. The robot moves by the joint control, and the measured values are given to wrench estimator which estimates contact wrench on parts without force sensors. Finally, the values are feedbacked to the stabilizer. This system does not support motions that bring multiple parts of the same limb into contact at the same time.

III. ONLINE MOTION STABILIZATION SYSTEM FOR DYNAMIC MULTI-CONTACT MOTION WITH IMPACT FORCE

In this section, we describe the online motion stabilization system for realizing dynamic multi-contact motion with impact force. The system must modify posture deviations due to adaptation to the environment by current-based torque control.

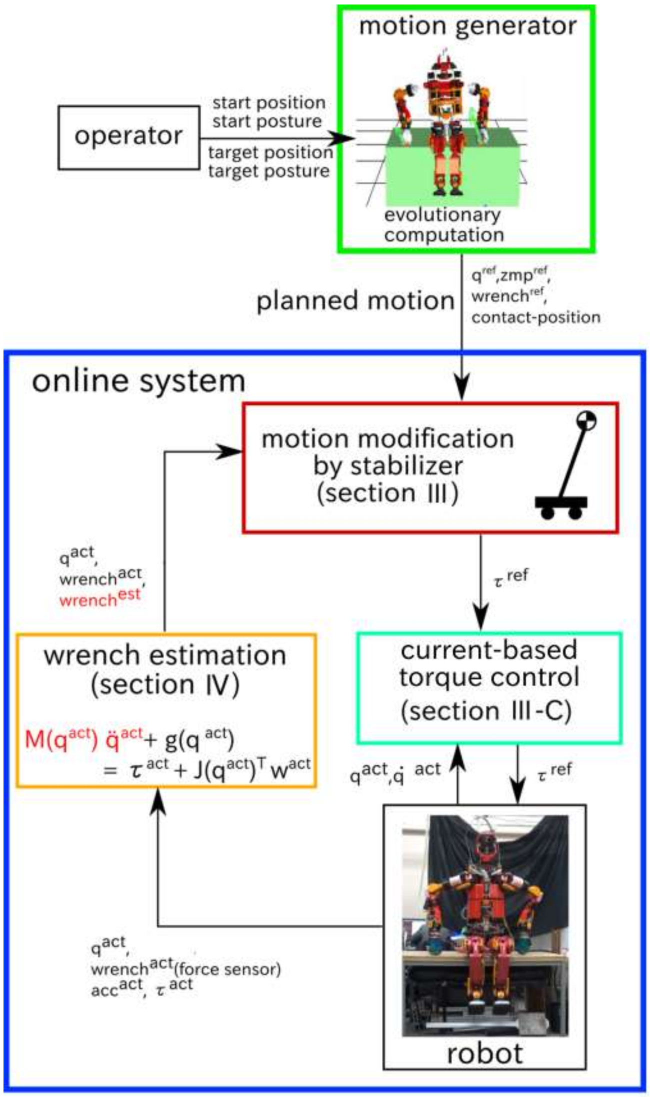

Fig. 2. Proposed dynamic multi-contact motion system overview. The online system consists of three components: Stabilizer (blown), joint controller (sky blue), and wrench estimator (orange).

Nozawa's stabilization method [1] by ZMP control which extended Kajita's method [18], consists of the following four parts.

1) measuring ZMP
2) modification of target ZMP based on linear inverted pendulum model
3) contact wrench distribution for multi-contact based on target contact wrenches of planned motion
4) compliant control according to the error between the target contact wrench and the actual contact wrench to realize distributed contact wrenches

In the proposed system, we applied estimated contact wrenches by section IV in 1), entered target contact wrenches at contact parts without force sensors from planned motion in 3), and replaced the compliant control with torque calculation by inverse dynamics for realizing distributed contact wrenches by current-based torque control in 4).

A. Measurement of ZMP Applying Estimated Contact Wrenches

Actual ZMP can be calculated by (1) if the contact wrenches at all contact points can be obtained by force sensors and contact wrench estimations. Because the moment around ZMP is zero, the sum of contact moment and cross product of the distance from ZMP and contact force at each contact point is zero around the axes other than the vertical axis. In this paper, contact wrenches at parts without force sensors are obtained by method described in section IV, and ZMP is measured by (1).

$$\sum_i \{(\boldsymbol{p}^{(i)}_{sen} - \boldsymbol{p}_{ZMP}) \times \boldsymbol{f}^{(i)}_{sen} + \boldsymbol{n}^{(i)}_{sen})\} + \sum_j \{(\boldsymbol{p}^{(j)}_{est} - \boldsymbol{p}_{ZMP}) \times \boldsymbol{f}^{(j)}_{est} + \boldsymbol{n}^{(j)}_{est})\} = \begin{bmatrix} 0 \\ 0 \\ n_z \end{bmatrix} \tag{1}$$

$\boldsymbol{p}_{ZMP}$ is the wanted ZMP. i and j are the number of contact points with and without force sensors respectively. $\boldsymbol{p}^{(i)}_{sen}$ are the positions of force sensors, and $\boldsymbol{p}^{(j)}_{est}$ are positions estimating contact points. $\boldsymbol{f}^{(i)}_{sen}$ and $\boldsymbol{n}^{(i)}_{sen}$ are contact forces and contact moments measured by force sensors respectively. $\boldsymbol{f}^{(j)}_{est}$ and $\boldsymbol{n}^{(j)}_{est}$ are contact forces and contact moments estimated by section IV respectively. n_z is moment occured around the vertical axis. In section VI-A and VI-C, the height of the ZMP in equation (1) was the midpoint of the contact point of both thighs when the both were in contact, the contact point of the right thigh when the right thigh was in contact and the left thigh was not, and the contact point of the left thigh otherwise.

The actual ZMP calculated by (1) is used in the target ZMP modification by the linear inverted pendulum model, and the contact wrenches are distributed in the next section to realize the modified target ZMP.

B. Distribution of Contact Wrenches for Dynamic Multi-contact Motion

By assuming that all the contact parts are known from the planned motion and entering target contact wrenches at contact parts without force sensors from planned motion to the contact wrench distributor by Nozawa's method [1], the contact wrenches can be distributed including parts without force sensors.

Specifically, according to the following formulae, contact wrenches are distributed by using a quadratic programming method.

$$\min \sum_i (\boldsymbol{w}^{(i)com}_{sen} - \boldsymbol{w}^{(i)ref}_{sen})^T \boldsymbol{W} (\boldsymbol{w}^{(i)com}_{sen} - \boldsymbol{w}^{(i)ref}_{sen}) + \sum_j (\boldsymbol{w}^{(j)com}_{est} - \boldsymbol{w}^{(j)ref}_{est})^T \boldsymbol{W} (\boldsymbol{w}^{(j)com}_{est} - \boldsymbol{w}^{(j)ref}_{est}) \tag{2}$$

$s.t.$

$$\boldsymbol{w}^{(k)com} = \left[\boldsymbol{f}^{(k)comT} \quad \boldsymbol{n}^{(k)comT}\right]^T \tag{3}$$

$$S_f \sum_k \boldsymbol{f}^{(k)com} = S_f \sum_k \boldsymbol{f}^{(k)ref} \tag{4}$$

$$S_m \sum_k \{(\boldsymbol{p}^{(k)} - \boldsymbol{p}^{ref^*}_{ZMP}) \times \boldsymbol{f}^{(k)com} + \boldsymbol{n}^{(k)com})\} = \boldsymbol{0} \tag{5}$$

k is the number of all contact points, which is the sum of i and j. $\boldsymbol{w}^{com}_{sen}$ is the computed wrench at the contact point with a force sensor by the distributor, and $\boldsymbol{w}^{ref}_{sen}$ is the reference wrench from planned motion at the contact point with a force sensor. $\boldsymbol{w}^{com}_{est}$ is the computed wrench at the contact point without a force sensor by the distributor, and $\boldsymbol{w}^{ref}_{est}$ is the reference wrench from planned motion at the contact point without a force sensor. $\boldsymbol{f}^{com}$ and $\boldsymbol{n}^{com}$ are computed forces and moments by the distributor, and $\boldsymbol{f}^{ref}$ is the reference forces from the planned motion. $\boldsymbol{p}^{ref^*}_{ZMP}$ is the position of the new reference ZMP computed by the linear inverted pendulum model, and $\boldsymbol{p}^{(k)}$ is the position of the k-th contact position. S_f,S_m are $l \times 3(0 < l \leq 3)$ matrix to determine the constraints applied to each element of force and moment. Experiments in section VI-A and section VI-C, we controlled f_z,n_x,n_y which contributes to vertical force.

C. Torque Calculation by Inverse Dynamics and Current-Based Torque Control

In order to realize the target contact wrenches distributed in section III-B even in parts without force sensors, we replaced compliant control according to the error between the target contact wrench and the actual contact wrench by principle of virtual work and inverse dynamics calculation for target torque by the following (6).

$$\begin{aligned} \boldsymbol{\tau}^{ref} = InverseDynamics(\boldsymbol{q}^{ref}, \dot{\boldsymbol{q}}^{ref}, \ddot{\boldsymbol{q}}^{ref}) \\ -\boldsymbol{J}(\boldsymbol{q}^{ref})^T \boldsymbol{w}^{com} \end{aligned} \tag{6}$$

For the principle of virtual work and inverse dynamics, the contact wrench is used from the distributed value ($\boldsymbol{w}^{com}$) at section III-B, and joint angles ($\boldsymbol{q}^{ref}$), angular velocities ($\dot{\boldsymbol{q}}^{ref}$), and angular accelerations ($\ddot{\boldsymbol{q}}^{ref}$) are used from the planned motion.

Based on these values, current-based torque control is applied at the joint level by the following (7).

$$i^{ref} = \frac{1}{K_t \cdot r} \tau^{ref} + P(q^{ref} - q^{act}) + D(\dot{q}^{ref} - \dot{q}^{act}) \tag{7}$$

i^{ref} is the target current to be calculated, K_t is the motor torque constant, r is the gear ratio, τ^{ref} is the target torque determined by the principle of virtual work and inverse dynamics, q^{ref}, $\dot{q}^{ref}$ are target angle and target angular velocity respectively, q^{act}, $\dot{q}^{act}$ are actual angle and actual angular velocity obtained by differentiating the measured angle respectively, and P, D are P gain and D gain respectively. The first term on the right side of equation (7) is a feedforward torque control term, and the second and the third terms on the right side are feedback control terms for joint angle and joint angular velocity respectively. PD control is necessary to prevent too large deviation from the target angle and the target angular velocity.

In the current-based torque control, since the current corresponding to the torque required to realize the target motion is stored in the first term on the right side, P gain and D gain can be reduced, which makes it possible to absorb impact force when in contact with the environment. In terms of each joint alone, this control would be a completely feed-forward torque control until the next target torque is given from the whole body control cycle if P gain and D gain were set to zero. In this paper, P gain and D gain were set small enough to absorb impact force. With this and the motion modification by the stabilizer described in this section, the target motion can be realized while allowing the contact errors with the planned motion to adapt to the environment.

IV. Online Estimation of Contact Wrenches

In this section, we describe the contact wrench estimation method for parts without force sensor.

Hiraoka's method [11] realized estimation of contact wrenches in parts without force sensors under the constraint that the motion is static and the position of the contact points are known. We extended this to dynamic conditions.

As a preparation, the equation of motion of the humanoid can be expressed as the following (8).

$$\begin{aligned} \boldsymbol{M}(\boldsymbol{q}^{act})\ddot{\boldsymbol{q}}^{act} + \boldsymbol{h}(\boldsymbol{q}^{act}, \dot{\boldsymbol{q}}^{act})\dot{\boldsymbol{q}}^{act} + \boldsymbol{g}(\boldsymbol{q}^{act}) \\ = \boldsymbol{\tau}^{act} + \boldsymbol{J}(\boldsymbol{q}^{act})^T \boldsymbol{w}^{act} \end{aligned} \tag{8}$$

n is the number of joints, m is the number of contact points, $\boldsymbol{q}^{act} \in \boldsymbol{R}^{6+n}$ is a vector of the root link position, the root link orientation, and the joint angles of the whole body. $\boldsymbol{\tau}^{act} \in \boldsymbol{R}^{6+n}$ is a vector of the driving torque of the virtual joint of the root link and the whole body joint, and $\boldsymbol{w}^{act} \in \boldsymbol{R}^{6m}$ is a vector of the contact wrenches at all contact points with the environment.

Hiraoka's method [11] applied $\dot{\boldsymbol{q}}^{act} = \boldsymbol{0}$ and $\ddot{\boldsymbol{q}}^{act} = \boldsymbol{0}$ to the equation (8) because of static motion. However, the first and the second terms on the left side of the equation (8) do not become 0 under dynamic motion. In order to extend estimation of contact wrenches to dynamic motion, it is required to consider these terms.

In this paper, we use estimated contact wrenches only for measuring ZMP and stabilizing motion in the online system. Therefore, the estimation does not require higher precision than necessary, and also the value of the second term on the left side of the equation (8), which is mainly due to the Coriolis force, is sufficiently smaller than the other terms, we approximated the second term to 0 in this paper. Then the equation of motion of the humanoid robot can be expressed as the following (9).

$$\boldsymbol{M}(\boldsymbol{q}^{act})\ddot{\boldsymbol{q}}^{act} + \boldsymbol{g}(\boldsymbol{q}^{act}) = \boldsymbol{\tau}^{act} + \boldsymbol{J}(\boldsymbol{q}^{act})^T \boldsymbol{w}^{act} \tag{9}$$

$\ddot{\boldsymbol{q}}^{act} \in \boldsymbol{R}^{6+n}$ is a vector of the root link acceleration, the root link angular acceleration, and the joint angular acceleration of the whole body joints. The root link acceleration is obtained from the mounted inertial measurement unit. The angular acceleration of the root link and each joint are obtained by differentiating twice the value obtained from the mounted inertial measurement unit and the encoder of each joint respectively. Since $\dot{\boldsymbol{q}}^{act}$ is not appeared in (9), we do not consider about the velocity of the root link. The values obtained from inertial measurement unit contains noise, so that a low-pass filter is applied. A low-pass filter is also applied when the values are differentiated.

Using the fact that (9) holds, let x be number of estimating contact points, $\boldsymbol{w}_{est}\in\boldsymbol{R}^{6x}$ be estimating contact wrenches, $\boldsymbol{w}_{sen}\in\boldsymbol{R}^{6(m-x)}$ be measured contact wrenches, and $\boldsymbol{\epsilon}$ be error on both sides, and express the equation as the following (10).

$$\begin{aligned}\boldsymbol{M}(\boldsymbol{q}^{act})\ddot{\boldsymbol{q}}^{act}+\boldsymbol{g}(\boldsymbol{q}^{act}) + \mathit{offset} \\ = \boldsymbol{\tau}^{act}+\boldsymbol{J}(\boldsymbol{q}^{act})^T \begin{pmatrix} \boldsymbol{w}_{est} \\ \boldsymbol{w}_{sen} \end{pmatrix} + \boldsymbol{\epsilon}\end{aligned} \quad (10)$$

Estimating $\boldsymbol{w}_{est}$ that minimizes $\boldsymbol{\epsilon}$ by quadratic programming within the range that satisfies the equation (10). *offset* is a constant vector to compensate for mass parameter errors, which determined by difference between both sides of (10) when all estimated contact points are not in contact.

The objective function at this time is the following (11).

$$\min_{\boldsymbol{w}_{est}} \|\boldsymbol{\epsilon}\|^2_{W_{eq}} + \|\boldsymbol{w}_{est}\|^2_{W_w} \quad (11)$$

The constraints are (10) and the following (12).

$$\boldsymbol{C}_w \boldsymbol{w}_{est} \leq \boldsymbol{d}_w \quad (12)$$

$\boldsymbol{C}_w$ and $\boldsymbol{d}_w$ are contact wrench constraints to prevent unrealistic estimates from the friction coefficient and link width.

V. Motion generation based on evolutionary computation

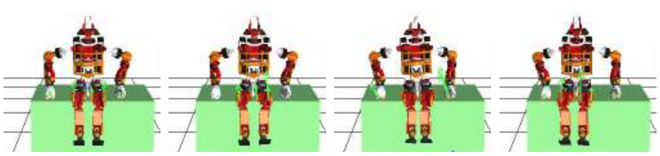

Fig. 3. Generated motion for the experiment moving rightward by sitting posture (section VI-C) by the evolutionary computation based on joint torque control.

As a motion planning for multi-contact motion which brings various parts of the body into contact with the environment, there are an optimization method based on an example of a human motion [21] and a method based on evolutionary computation [22]. We extended Noda's method by evolutionary computation [22] to behavior of torque control in order to realize dynamic motion by torque control. In the motion planning by the evolutionary computation [22], the starting position and posture of the robot and the target position and posture of the robot are required to be set. The motion is searched by simulating each interpolated target joint angle trajectories by evolutionary computation.

In this paper, since experiments are conducted by current-based torque control, simulations of the motion planning should also be conducted with the behavior of torque control. Therefore, in addition to target joint angle trajectories, we added the target joint torque trajectories as the variables searched by the evolutionary computation. By combining these trajectories, we generated motion considering behavior of the torque control.

VI. Experiments and Evaluations

A. Functional Experiment for Posture Stabilization

In this experiment, we assessed the posture stabilization capability by the proposed online system (Fig. 2) in the multi-contact posture. For the real robot JAXON in a sitting posture which the hands and the back of the thighs were in contact with the environment and the feet were floating like Fig. 4, we pushed its body from the front to the back as a disturbance to confirm that the target zmp was modified by the stabilization control to balance. In order to balance properly, it is required that motion modification by stabilizer and wrench estimation in Fig. 2 works at enough degree of correctness. The posture stabilization is important because the robot can fall back or forward by external forces or changes in posture when moving.

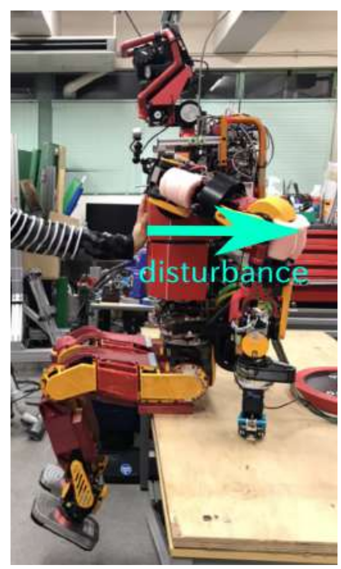

Fig. 4. JAXON is pushed backward as a disturbance under multi-contact sitting posture. This is the experiment for assessing the capability of motion modification by the proposed online system.

We pushed the robot body from front to back at around 2.5 [s] and 8.5 [s] in Fig. 5. When the robot was pushed, both the measured zmp and the modified zmp changed, and it can be seen that the measured zmp was stabilized by following the modified zmp. At 2.5 [s], not only the measured zmp but also the modified zmp greatly changed the value, and stabilized at around 6.5 [s]. From 6.5 [s] to 8.5 [s], although there was

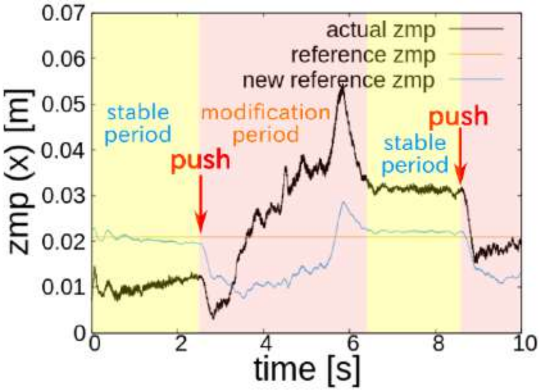

Longitudinal direction of zmp

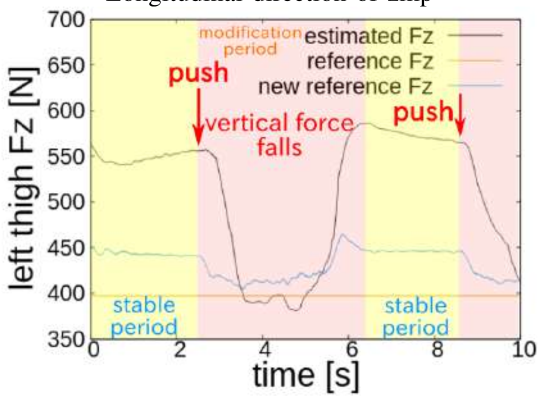

Vertical force at left thigh

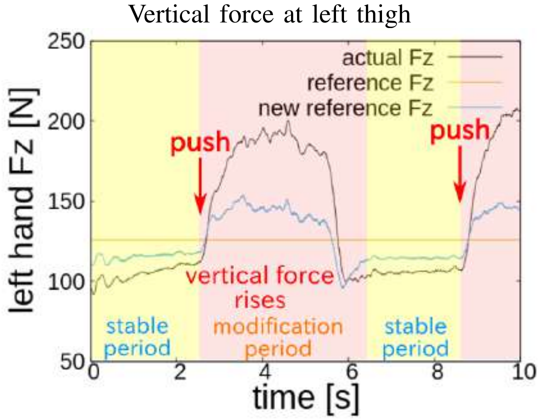

Vertical force at left hand

Fig. 5. Graph of zmp and vertical force at the experiment of pushing JAXON sitting on the table (Fig. 4).

an almost constant difference between the measured zmp and the modified zmp, it can be said that the actual zmp behavior is stable following the modified zmp because modified zmp hardly changed relative to target zmp and the measured zmp is also hardly changed. Regarding the difference of this constant value, it is conceivable that it is caused by robot modeling errors.

As for the vertical force at the back of the thigh, the modified target vertical force and the actual vertical force decreased immediately after 2.5 [s] and 8.5 [s] when the external force was applied. On the other hand, the modified target vertical force and the actual vertical force increased at the hands immediately after the external force was applied. Since both the modified target vertical force and the actual vertical force at thighs and hands returned to the same value as the original value while zmp was stabilized, it can be evaluated that the proposed online system modifies the target contact wrench appropriately against disturbance and it stabilizes zmp in the multi-contact posture.

B. Functional Experiment for Impact Force Absorption

t = 0.00 [s] t = 0.50 [s] t = 1.00 [s]

Fig. 6. Appearance of the experiment to give impact force on the left hand of JAXON. The experiment is for assessing efficiency of impact abosorption capacity by the current-based torque control system.

In this experiment, we assessed the impact force absorption capability by using current-based torque control as joint control in Fig. 2. For each of the current-based torque control and compliant control according to the error between the target contact wrench and the actual contact wrench (called impedance control in Fig. 7), we hit a weight of 15 [kg] on the hand of JAXON equipped with a force sensor (Fig. 6), and compared the impact force arose at that time.

In order to give as equal impact force as possible, the weight was suspended with a string so that the weight contacts the left hand when passing the lowest point of the pendulum, and released from the same position. In addition, since the shape of the robot hand has many irregularities and the contact state was not stable, it was removed and the plane of the force sensor was used as the hand.

The maximum value of the impact force by the compliant control was about 350 [N], and by the current-based torque control was about 300 [N] (Fig. 7). Therefore, the impact force was about 14 [%] smaller when the current-based torque control was applied, and is considered effective for impact force absorption.

Since we didn't apply Nagamatsu's method [16] to compensate for energy loss due to friction arose in gears in this paper, it is considered that the impact force absorption capability of the current-based torque control is further improved by incorporating this method into the system.

C. Experiments of Locomotion to Sideway in a Sitting Posture

For integrated experiments, we conducted experiments of locomotion to sideway in a sitting posture by a JAXON

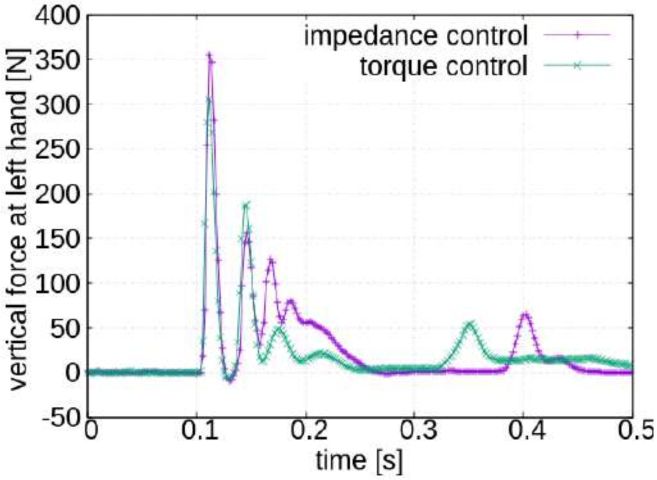

Fig. 7. Graph of the vertical force at the left hand of JAXON.

robot in which impact force occurs on the back of the thighs which have no force sensors (Fig. 9 and video is also attached) as an example of dynamic multi-contact motion with impact force. We used the method described in section V for motion planning, and Fig. 3 is the planned motion for this experiment. The contact points for estimating contact wrenchs were given from the motion generator.

The motion was started from about 0.2 [s]. From the graph of the target vertical force and the measured or the estimated vertical force in Fig. 8, it is confirmed that the contact wrench and the contact timing are different between the planned motion and the actual motion. In addition, it is also confirmed that the differences between target joint angles and the actual joint angles are large from the timing when the misalignment of contact states occur.

Thus, it can be considered that the robot was able to realize a dynamic multi-contact motion with impact force involving contacts with parts without force sensors by adapting to the environment and tolerating errors of the contact wrench and the contact timing.

On the other hand, as shown in Table I, the actual movement distance was smaller than the planned motion. The causes of this is considered to be the difference of friction coefficient between the simulation and the real environment, which arose slip of hands when pushing the environmet and the difference of friction force when the legs moved. The slight difference of initial posture from the planned motion due to adaptation to the environment by torque control is also considered to be the cause. The proposed system cannot tolerate and modify these errors so far.

TABLE I

MOVED DISTANCE OF JAXON AT THE EXPERIMENT OF MOVING RIGHTWARD BY SITTING POSTURE.

	simulation	real robot
moved distance	10 [cm]	2.5 [cm]

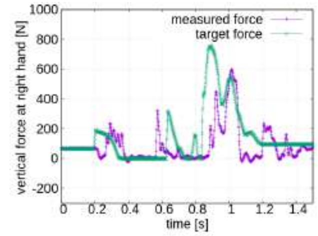

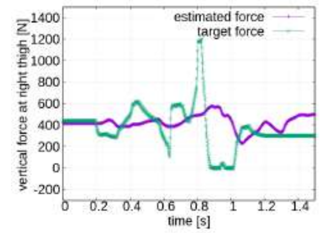

vertical force at right arm vertical force at right thigh

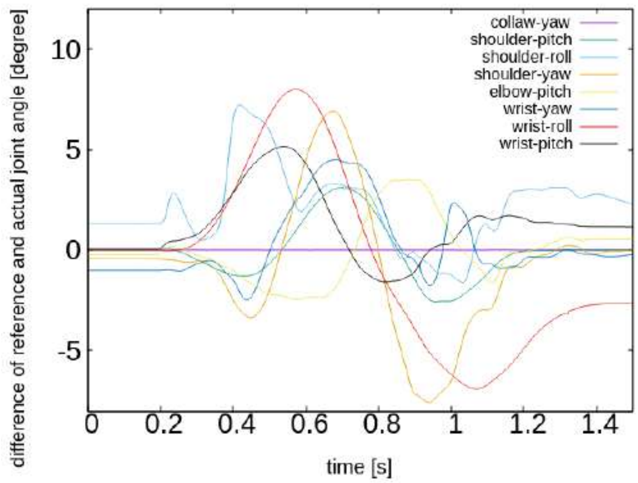

Differences between reference and actual joint-angles of right arm

Fig. 8. Graph of zmp, vertical force, differences of joint angles at the experiment of pushing JAXON sitting on the table.

VII. CONCLUSIONS

In this paper, we proposed online system for realizing dynamic motion including contact with impact force and described its configuration. Although it is possible to adapt to the environment against impact force for the whole body including parts without force sensors by applying current-based torque control as joint control, there was a problem that the actual motion was deviated from the planned motion due to adaptation to the environment. Therefore, we introduced the stabilization system that modifies the motion deviation due to the torque control and realizes the target motion by estimating contact wrenchs at parts without force sensors which are required for the stabilization system.

As a result, we realized the system for dynamic multi-contact motion with impact force which tolerates errors of the contact wrench and the contact timing, and demonstlated by experiments of locomotion in the sitting posture by a JAXON robot in which an impact force occurs on the back of the thighs without force sensors. The system cannot torelate and modify errors such as difference of friction coefficient between the simulation and the real environment, or deviation of the initial robot posture due to torque control. Systems that modify planned motion in the real environment by feeding back the state of the environment or the result of the motion once conducted in the actual environment are required.

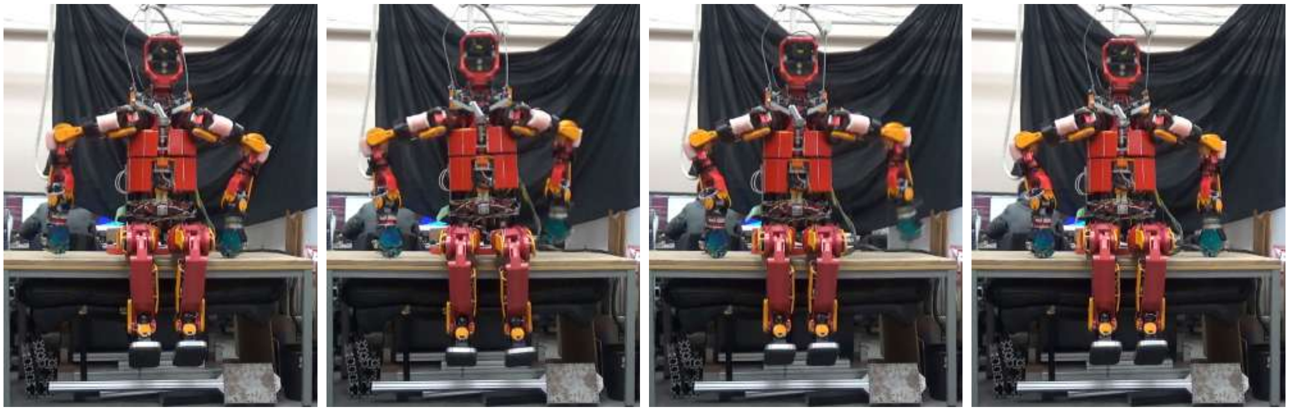

t = 0.00 [s] t = 0.33 [s] t = 0.67 [s] t = 1.00 [s]

Fig. 9. Appearance of JAXON moving rightward by sitting posture.

REFERENCES

[1] Shunichi Nozawa, Shintaro Noda, Masaki Murooka, Kei Okada, and Masayuki Inaba. Online estimation of object-environment constraints for humanoid motion planning applicable to movable stepladder climbing. *2017 IEEE International Conference on Robotics and Automation (ICRA)*, pp. 1291 – 1298, 7 2017.

[2] Shintaro Noda, Masaki Murooka, Shunichi Nozawa, Yohei Kakiuchi, Kei Okada, and Masayuki Inaba. Generating whole-body motion keep away from joint torque, contact force, contact moment limitations enabling steep climbing with a real humanoid robot. *2014 IEEE International Conference on Robotics and Automation (ICRA)*, pp. 1775–1781, 2014.

[3] Masao Kanazawa, Shunichi Nozawa, Yohei Kakiuchi, Yoshiki Kanemoto, Mitsuhide Kuroda, Kei Okada, Masayuki Inaba, and Takahide Yoshiike. Robust vertical ladder climbing and transitioning between ladder and catwalk for humanoid robots. *2015 IEEE/RSJ International Conference on Intelligent Robots and Systems (IROS)*, pp. 2202–2209, 2015.

[4] Joris Vaillant, Abderrahmane Kheddar, Herv Audren, Franois Keith, Stanislas Brossette, Kenji Kaneko, Mitsuharu Morisawa, Eiichi Yoshida, and Fumio Kanehiro. Vertical ladder climbing by the hrp-2 humanoid robot. *2014 IEEE-RAS International Conference on Humanoid Robots*, pp. 671–676, 2014.

[5] Kensuke Harada, Hirohisa Hirukawa, Fumio Kanehiro, Kiyoshi Fujiwara, Kenji Kaneko, Shuuji Kajita, and Masaru Nakamura. Dynamical balance of a humanoid robot grasping an environment. *Intelligent Robots and Systems, 2004. (IROS 2004).*, pp. 1167 – 1173, 10 2004.

[6] Masahiro Bando, Masaki Murooka, Shunichi Nozawa, Kei Okada, and Masayuki Inaba. Walking on a steep slope using a rope by a life-size humanoid robot. *2018 IEEE/RSJ International Conference on Intelligent Robots and Systems (IROS)*, pp. 705–712, 2018.

[7] Eisoku Kuroiwa, Kunio Kojima, Takuya Nakaoka, Shunichi Nozawa, Kei Okada, and Masayuki Inaba. Realization of Multi Gait Motion based on the Extension from Biped Walking to Walking under Arm/Leg Coordination of Humanoids. In *Proceedings of the 2014 JSME Conference on Robotics and Mechatronics (in Japanese)*, 2014.

[8] Bernd Henze, Alexander Dietrich, Mximo A. Roa, and Christian Ott. Multi-contact balancing of humanoid robots in confined spaces: Utilizing knee contacts. *Intelligent Robots and Systems, 2017. (IROS 2017).*, pp. 697 – 704, 9 2017.

[9] Bernd Henze, Mximo A. Roa, and Christian Ott. Passivity-based whole-body balancing for torque-controlled humanoid robots in multi-contact scenarios. *The International Journal of Robotics Research 2016*, pp. 1522–1543, 2016.

[10] M. P. Polverini, A. Laurenzi, E. M. Hoffman, F. Ruscelli, and N. G. Tsagarakis. Multi-contact heavy object pushing with a centaur-type humanoid robot: Planning and control for a real demonstrator. *IEEE Robotics and Automation Letters*, Vol. 5, No. 2, pp. 859–866, 2020.

[11] Naoki Hiraoka, Masaki Murooka, Shintaro Noda, Kei Okada, and Masayuki Inaba. Online Generation and Control of Quasi-Static Multi-contact Motion with PWT Jacobian Matrix and Contact Wrench Estimation. *25th Robotics Symposia (in Japanese)*, 2020.

[12] Shuuji Kajita, Takeshi Sakaguchi, Shin'ichiro Nakaoka, Mitsuharu Morisawa, Kenji Kaneko, and Fumio Kanehiro. Quick squatting motion generation of a humanoid robot for falling damage reduction. *2017 IEEE International Conference on Cyborg and Bionic Systems (CBS)*, pp. 45–49, 2017.

[13] Boston Dynamics. atlas. https://www.bostondynamics.com/atlas.

[14] Texas Instruments. Ads1208. https://www.ti.com/product/ADS1208.

[15] Texas Instruments. Amc1203. https://www.ti.com/product/AMC1203.

[16] Yuya Nagamatsu, Takuma Shirai, Hiroto Suzuki, Yohei Kakiuchi, Kei Okada, and Masayuki Inaba. Distributed torque estimation toward low-latency variable stiffness control for gear-driven torque sensorless humanoid. *2017 IEEE/RSJ International Conference on Intelligent Robots and Systems (IROS)*, p. 5239 5244, 9 2017.

[17] Hiroshi Kaminaga, Tianyi Ko, Satoshi Yorita, Shunsuke Sato, Ryo Masumura, Mitsuo Komagata, Tatsuya Ishikawa, Taira Miyatake, and Yoshihiko Nakamura. Enhancement of mechanical strength, computational power, and heat management for fieldwork humanoid robots. *2016 IEEE-RAS 16th International Conference on Humanoid Robots (Humanoids)*, pp. 786–793, 2016.

[18] Shuuji Kajita, Mitsuharu Morisawa, Kanako Miura, Shinichiro Nakaoka, Kensuke Harada, Kenji Kaneko, Fumio Kanehiro, and Kazuhito Yokoi. Biped walking stabilization based on linear inverted pendulum tracking. *Intelligent Robots and Systems, 2010. (IROS 2010).*, pp. 4489 – 4496, 10 2010.

[19] Alessandro De Luca and Raffaella Mattone. Sensorless robot collision detectionand hybrid force/motion control. In *Proceedings of the 2005 IEEE International Conference on Robotics and Automation*, pp. 999–1004, 2005.

[20] Lucas Manuelli and Russ Tedrake. Localizing external contact using proprioceptive sensors: The contact particle filter. *2016 IEEE/RSJ International Conference on Intelligent Robots and Systems (IROS)*, pp. 5062–5069, 2016.

[21] Pavan Kanajar, Darwin G. Caldwell, and Petar Kormushev. Climbing over large obstacles with a humanoid robot via multi-contact motion planning. *2017 26th IEEE International Symposium on Robot and Human Interactive Communication (RO-MAN)*, pp. 1202–1209, 2017.

[22] Shintaro Noda, Yohei Kakiuchi, Hiroki Takeda, Kei Okada, and Masayuki Inaba. Experiments on knee-contact motion and transition between foot-contact state towards whole-body multi-contact behavior. *2018 18th IEEE-RAS International Conference on Humanoid Robots*, pp. 761–767, 2018.